


Underwater Imaging by Suppressing the Backscattered Light Based on Mueller Matrix

Hongyuan Wang , Jiaqi Li , Haofeng Hu , Junfeng Jiang , Xiaobo Li , Kan Zhao, Zhenzhou Cheng , Mei Sang , and Tiegeng Liu 

Abstract—Polarimetric imaging is an effective way for enhancing the image quality in underwater environments. Previous polarization-based methods for underwater imaging actually involve both optical and digital processing, while compared with digital processing, the importance of the optical method is not clear. In this paper, we propose a polarimetric method for underwater imaging based on the Mueller imager. In this method, in order to optimally filter out the backscattered light and enhance the image quality, the polarization states of illumination light together with the polarization filter in front of the camera are synergistically modulated in an optical way. In other words, the quality of images captured by the camera can be directly improved without any digital processing. A series of experimental results show the effectiveness of the proposed method, which indeed verifies its superiority in scattering media.

Index Terms—Polarimetric imaging, underwater imaging, Mueller matrix, scattering media.

I. INTRODUCTION

THE image quality in underwater environments can be severely degraded due to the scattering by the particles existing in water [1]–[4]. The backscattered light (veiling light) is partially polarized [3]–[5], and thus in principle, polarimetric imaging can effectively suppress the backscattered light and enhance the image quality.

Up to now, various polarization-based methods for underwater imaging have been developed to enhance the quality of underwater images by suppressing the backscattered light and enhancing the object radiance [6], [7]. However, most previous polarimetric recovery methods in fact involve digital processing

and are based on the polarization imaging model in scattering media [8], [9]. This could induce considerable image distortion (such as the uneven distribution of light intensity) [10], and in addition, the mixture of digital processing makes that the contribution of optical processing is unclear. On the other hand, previous methods are based on the Stokes configuration, which rarely consider the modulation of the illumination light [11], [12], and thus the power of the polarimetric method for underwater imaging is not sufficiently utilized yet.

In this paper, based on the Mueller imaging configuration, we propose a method to suppress the backscattered light and enhance the underwater image quality in an optical way without digital processing. We first analyze the relationship between the polarization states of the backscattered light and the illumination beam. Based on this relation, we modulate the polarization state analyzer in front of the camera to filter out the backscatter in an optimal way. By this method, the quality of the image captured by the camera can be directly improved, in other words, the camera direct shows the “clear and recovered underwater images”. We perform several experiments to verify the effectiveness of our method, and we also compare the performance of the proposed method with those of other methods.

II. THEORY

The typical model of imaging in the scattering media shows that the light obtained by the camera includes two parts [13]. The first one is the direct transmission referring to the target signal, which is attenuated due to the absorption and scattering. The second one is the backscattered light, which comes from the light scattered towards the camera by scattering particles in water [14]–[17]. In fact, the decay of image quality in the underwater scenario is mainly due to the backscattered light received by the camera. Therefore, suppressing the backscattered light is essential for underwater imaging [4]–[7].

In fact, the backscattered light is partially polarized [3], [13], and its polarization state depends on the polarization states of the illumination light and the turbidity of the medium [12], [18], [19]. Therefore, it is possible to suppress the backscattered light by adjusting the polarization states of polarization state generation (PSG) and polarization state analysis (PSA). By adjusting optical elements in PSG, we can obtain a specific polarized illumination with the Stokes vector of \mathbf{S}^{in} [29], which

Manuscript received May 29, 2021; revised June 22, 2021; accepted June 30, 2021. Date of publication July 2, 2021; date of current version August 5, 2021. This work was supported by the National Natural Science Foundation of China under Grants 61775163 and 62075161, and in part by the Guangxi Special Fund Project for Innovation-driven Development (GuikeAA21077008). (Hongyuan Wang and Jiaqi Li contributed equally to this work.) (Corresponding authors: Haofeng Hu and Junfeng Jiang.)

Hongyuan Wang, Jiaqi Li, Haofeng Hu, Junfeng Jiang, Kan Zhao, Zhenzhou Cheng, Mei Sang, and Tiegeng Liu are with the School of Precision Instrument and Opto-electronics Engineering, Tianjin University, Tianjin 300072, China, and also with the Key Laboratory of Opto-electronics Information Technology, Ministry of Education, Tianjin 300072, China (e-mail: wanghongyuan@tju.edu.cn; lj997995@tju.edu.cn; haofeng_hu@tju.edu.cn; jiangjfxu@tju.edu.cn; dakanxia3434@163.com; zhenzhoucheng@tju.edu.cn; m_sang@tju.edu.cn; tgliu@tju.edu.cn).

Xiaobo Li is with the Department of Mechanical and Automation Engineering, The Chinese University of Hong Kong, Shatin, N.T., Hong Kong, SAR 999077, China (e-mail: lixiaobo@cuhk.edu.cn).

Digital Object Identifier 10.1109/JPHOT.2021.3094359

can be represented by the azimuth α and the ellipticity ε as:

$$\mathbf{S}^{in} = s_0^{in} \begin{bmatrix} 1 & & & \\ & P \cos 2\alpha \cos 2\varepsilon & & \\ & P \sin 2\alpha \cos 2\varepsilon & & \\ & & & P \sin 2\varepsilon \end{bmatrix}^T = s_0^{in} \begin{bmatrix} 1 \\ P \cos 2\alpha \cos 2\varepsilon \\ P \sin 2\alpha \cos 2\varepsilon \\ P \sin 2\varepsilon \end{bmatrix} \quad (1)$$

where s_0^{in} denotes the intensity of the illumination light, $\mathbf{s} = [s_1^{in}, s_2^{in}, s_3^{in}]$ is the normalized Stokes vector, and P is the degree of polarization (DoP). Assuming that the Mueller matrix of the turbid water is M , the Stokes vector of the backscattered light \mathbf{S}^{back} is thus equal to:

$$\mathbf{S}^{back} = [s_0^{back}, s_1^{back}, s_2^{back}, s_3^{back}]^T = M \cdot \mathbf{S}^{in} \quad (2)$$

Generally speaking, when the DoP of backscattered light is higher, a higher proportion of backscattered light can be blocked by the PSA. Therefore, in order to suppress the backscattered light in an optimal way, one has to maximize the DoP of the backscattered light by choosing an optimal set of azimuth and ellipticity ($\alpha_{opt}, \varepsilon_{opt}$) corresponding to the polarized illumination light, which can be expressed by:

$$(\alpha_{opt}, \varepsilon_{opt}) = \arg \max_{(\alpha, \varepsilon)} \{P_{back}(M, \alpha, \varepsilon)\} \quad (3)$$

where

$$P_{back}(M, \alpha, \varepsilon) = \frac{1}{s_0^{back}} \left[(s_1^{back})^2 + (s_2^{back})^2 + (s_3^{back})^2 \right]^{\frac{1}{2}} \\ = \frac{1}{\sum_{j=0}^3 M_{0j} s_j^{in}(\alpha, \varepsilon)} \left\{ \sum_{i=1}^3 \sum_{j=0}^3 [M_{ij} s_j^{in}(\alpha, \varepsilon)]^2 \right\}^{\frac{1}{2}} \quad (4)$$

In (4), $s_j^{in}(\alpha, \varepsilon)$ means the Stokes parameters depending on the parameters (α, ε) . It can be seen in (4) that, the DoP of the backscattered light is a function of azimuth and ellipticity (α, ε) of the illumination light and the Mueller matrix of the turbid water. Indeed, when DoP reaches the maximum value, the optimal set $(\alpha_{opt}, \varepsilon_{opt})$ can be calculated by the derivative analysis for a given Mueller matrix:

$$\frac{\partial P_{back}(M, \alpha, \varepsilon)}{\partial \alpha} = 0 \text{ and } \frac{\partial P_{back}(M, \alpha, \varepsilon)}{\partial \varepsilon} = 0 \quad (5)$$

In fact, the Stokes vector \mathbf{S}^{back} can be decomposed into the Stokes vector of the polarized light \mathbf{S}_p^{back} and that of the unpolarized light \mathbf{S}_u^{back} , which can be expressed as:

$$\mathbf{S}_p^{back} = [P_{back} s_0^{back}, s_1^{back}, s_2^{back}, s_3^{back}]^T \\ \mathbf{S}_u^{back} = [(1 - P_{back}) s_0^{back}, 0, 0, 0]^T \quad (6)$$

Let \mathbf{A} denote the polarization eigenvector of PSA. If \mathbf{A} and \mathbf{S}_p^{back} are orthogonal, then the backscattered light can be blocked by PSA to the most extend. For this purpose, the eigenvector of PSA should satisfy:

$$\mathbf{A} = \frac{1}{P_{back} s_0^{back}} [P_{back} s_0^{back}, -s_1^{back}, -s_2^{back}, -s_3^{back}]^T \quad (7)$$

According to (3) and (7), a clear image with the maximal suppression of the backscattered light can be obtained by adjusting the states of PSA and PSG synergistically.

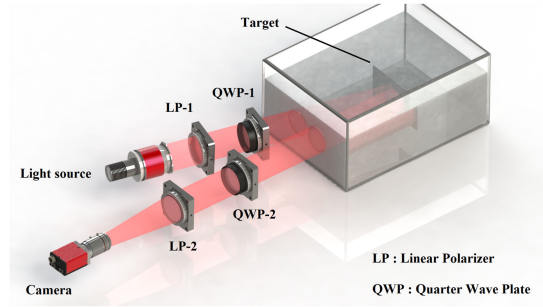


Fig. 1. Experimental setup of underwater imaging based on the Mueller matrix.

It is well known that the typical PSA consists of a linear polarizer (LP) and a quarter wave plate (QWP) [20], [21]. Let the orientation of the LP be γ and the orientation of the QWP be θ . The eigenvector of PSA can be expressed by the orientations of the LP and QWP as:

$$\mathbf{A} = \begin{bmatrix} 1 \\ \cos^2(2\theta) \cos(2\gamma) + \sin(2\theta) \cos(2\theta) \sin(2\gamma) \\ \sin(2\theta) \cos(2\theta) \cos(2\gamma) + \sin^2(2\theta) \sin(2\gamma) \\ -\sin(2\theta) \cos(2\gamma) + \cos(2\theta) \sin(2\gamma) \end{bmatrix} \quad (8)$$

Then the image captured by the camera is given by [22]:

$$I(x, y) = \frac{1}{2} \mathbf{A}^T \mathbf{S}(x, y) = \frac{1}{4} \{ 2s_0(x, y) \\ + s_1(x, y) [\cos(4\theta - 2\gamma) + \cos 2\gamma] \\ + s_2(x, y) [\sin(4\theta - 2\gamma) + \sin 2\gamma] \\ - 2s_3(x, y) \sin(2\theta - 2\gamma) \} \quad (9)$$

III. EXPERIMENTAL RESULTS AND DISCUSSION

The Mueller polarimetric imaging setup for this work is shown in Fig. 1. The targets (a plastic sticker and a ‘‘TJU’’ black handwriting on a white plastic board) are put inside a transparent PMMA tank (65 × 25 × 25 cm) filled with water, and we make the water turbid by blending the clear water with milk. Semi-skimmed milk contains more fat globules and results in a Mie scattering system, while skimmed milk consists mainly of small particles and results in a predominantly Rayleigh scattering system. In Rayleigh regime, the characteristic length of depolarization for incident linearly polarized light exceeds it for incident circularly light, while the opposite is true for Mie regime [30]. Long-term underwater experiments proved that the scattering system formed by milk is similar to the scattering system in seawater environments, and thus in this paper, the semi-skimmed milk is mixed into the water to make the scattering properties of the medium in the experiment similar to the real seawater. Semi-skimmed milk is composed of spherical particles of 0.04-20 μm . The scattering coefficient for semi-skimmed milk is $1.40c \text{ cm}^{-1}$, where c is the concentration of milk in water [23]. The scattering coefficient of turbid water decreases as the wavelength increases in the visible light range. In order to reduce the scattering effect, we employ a Light-Emitting Diode

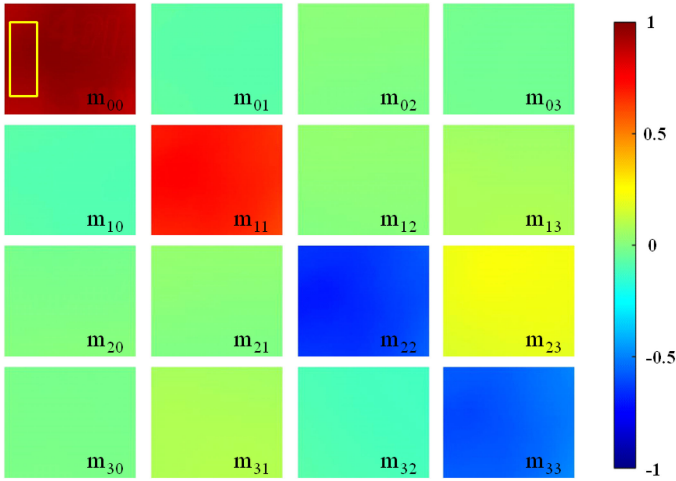


Fig. 2. Mueller matrix image of the scene in turbid water. The background region is marked by the yellow rectangle in m_{00} .

(LED) with the central wavelength of 625nm to illuminate the scene, and the angle between the light emission and camera axis is 21° . Both PSG and PSA are composed of one LP and one QWP. The states of PSG and PSA can be modulated by adjusting the orientations of LPs and QWPs. The images are taken by a monochrome CCD camera (AVT Stingray F-033B, with a resolution of 656×492 and a bit depth of 8-bit).

It should be noted that, although the optical elements in Fig. 1 are the same as these in reference [12], there are essential differences between these two methods. This is because in order to filter the backscattered light to the most extent, both the states of PSG and PSA in this work are optimized to maximize the DoP value of the backscattered light, while these in Ref. [12] are just used to generate the circularly polarized illumination and to measure the Stokes vector of the reflected light from the scene.

With the experimental setup shown in Fig. 1, we measure the Mueller matrix of the scene in turbid water, as shown in Fig. 2. The concentration of milk in water is 0.62 g/L. It can be seen that the absolute values of the Mueller elements on the diagonal are relatively greater, which indicates that depolarization is the dominant mechanism in turbid water due to the scattering. In addition, due to the scattering by the turbid water, it is difficult to distinguish the details of the object in the Mueller images in Fig. 2.

In order to investigate the relation between the DoP of the backscattered light and the polarization state of the incident light, we calculate the values of DoP in the background region without the target (shown as the yellow rectangle in Fig. 2) at different states of PSG according to the Mueller matrix in Fig. 2. The result is shown in Fig. 3, in which the polarization state (Stokes vector) of the incident light depends on the azimuth and ellipticity of its Stokes vector. It can be seen from Fig. 3 that the DoP of the backscattered light changes considerably with the polarization state of the incident light. According to the color bar in Fig. 3, it can be seen that the variation of the DoP of the backscattered light is between 0.6 and 0.8. It means that the backscattered

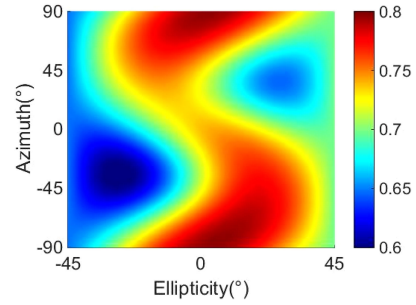


Fig. 3. Variation of DoP with the azimuth and the ellipticity of PSG at the concentration of milk in the water of 0.62 g/L.

light has a high DoP in the case of polarized illumination, and its DoP changes significantly with the polarization state of the incident light, which makes the proposed method more effective. The purpose of adjusting the polarization state of PSG is to get the maximum DoP, and the corresponding azimuth and ellipticity are about $(-87.05^\circ, 4.67^\circ)$ in this work. In practice, the position at the target is clearly defined, and other positions can be recognized as the background light position. If the region of the background is not clear, the region of the target is also not clear, and in this case, the average of the brightest 0.1% part in the image can be selected as the average of the background light [24], which can also achieve a relatively good scattering suppression effect.

By adjusting the state of PSA to the optimal one described in (7), we can filter out the backscattered light to the most extent, and the image directly captured by the camera is shown as “Mueller Step-1” in Fig. 4(a). The “Raw image” is taken in turbid water without any polarized device by removing PSG and PSA, while the “Clear image” is taken in clear water without PSG and PSA. It can be seen that compared with the intensity image in turbid water, which is the “Raw image” shown in Fig. 4(a), the image quality of our method shown in the middle of Fig. 4(a) is significantly improved. It demonstrates that the backscattered light can be effectively suppressed by the polarization-based optical filters, and thus the contribution of polarization to underwater imaging is demonstrated to be significant.

In addition, we also compare our restoration result with the traditional polarimetric underwater imaging method proposed by Schechner [3], as “Schechner Step-1” shown in the right of Fig. 4(a). It can be seen that the performance of our method is better than that of the traditional polarimetric imaging method. However, it should be noted that, although the traditional polarimetric method is based on the physical model, it actually involves digital processing to enhance the quality of the image, while our method improves the image quality only by optical filtering. Besides, in the first step, since our method outputs the improved images without any post-processing, it indeed corresponds to a vision enhancement system. This is also an important difference compared with the method in Ref. [12], which actually focuses on processing multi-images to enhance the image quality and needs more acquisitions to measure the Stokes vector.

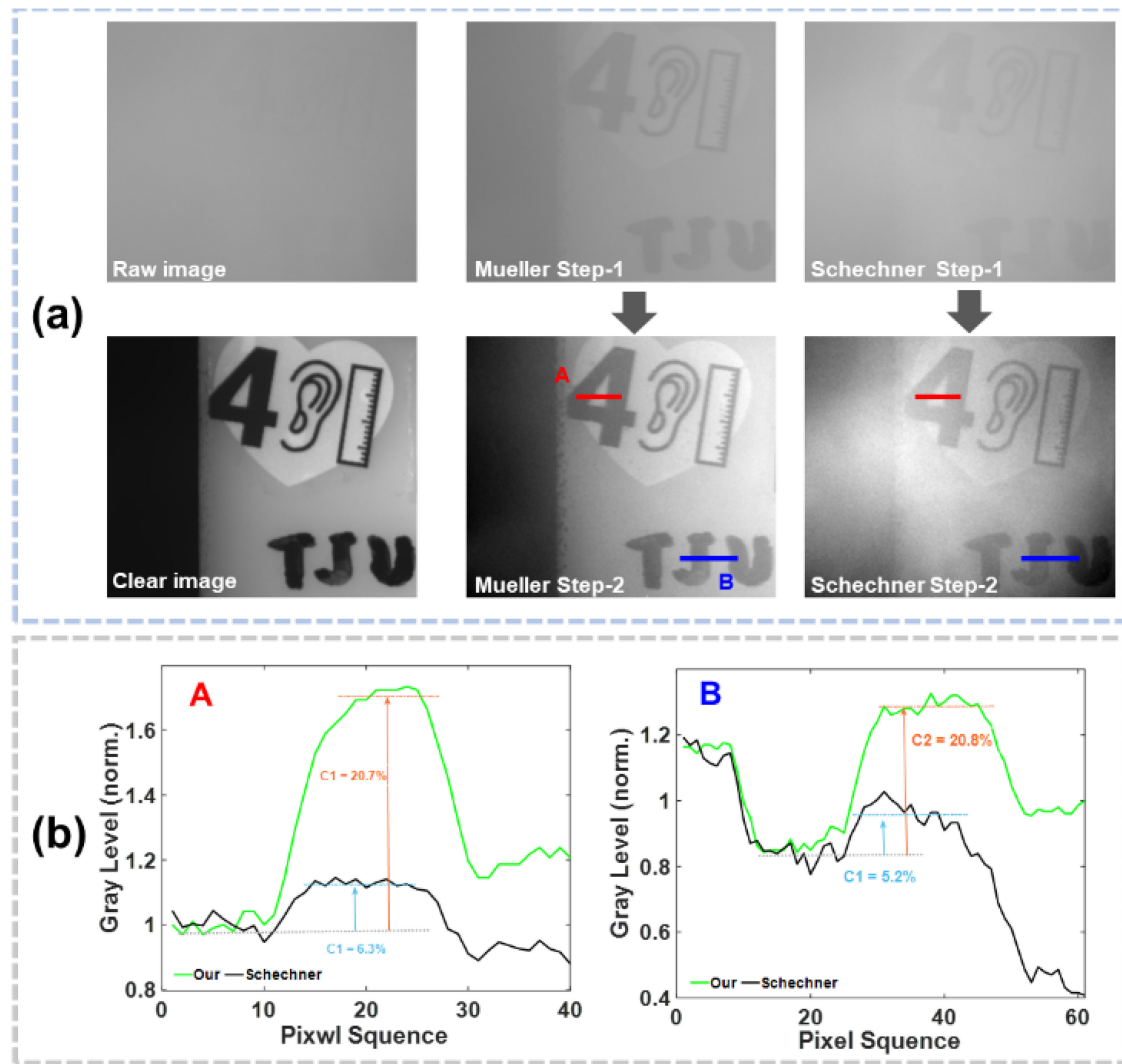


Fig. 4. (a) Comparison of different images in turbid water; (b) Intensity level at the indicated places. Step-1 indicates the processing by our method or by Schechner's method, while Step-2 indicates the consequent histogram stretching.

Moreover, considering that the outputs of the proposed Mueller imager have less image distortion, the technique of image processing can thus be applied to further enhance the image quality. We perform the histogram stretching [4], which is a typical and simple way of image enhancement with the linear operation, for these images in the first row of Fig. 4(a). The results are shown in the second row of Fig. 4(a). It can be seen that after histogram stretching, the image quality can be further improved. However, it can be seen from the result of "Schechner Step-2" in Fig. 4(a) that the brightness of the image is not uniform. For example, the central left part of the image "Schechner Step-2" is obviously brighter. This is originated from the fact that digital processing is involved in the traditional polarimetric image recovery method which inevitably causes image distortion. While the image quality for our result is better with clearer vision and uniform brightness. This is because the optical filtering without digital processing leads to a lower image distortion, which lays a better foundation for the subsequent image processing.

Of course, it needs to be clarified that we employ histogram stretching in this work, which is the simplest image processing method, as an example to illustrate that image processing can further enhance the image quality. If we employ more advanced image processing methods, such as dark channel prior [24] and Realization of the Contrast Limited Adaptive Histogram Equalization (CLAHE) [25], the image quality can be even better than those in the last row of Fig. 4(a). In addition, we choose two regions (A and B) in the image in Fig. 4(a) to compare the image quality for different methods in more detail, and the gray levels along line A and line B are shown in Fig. 4(b). It can be seen that our method has a greater magnitude of gray level variation, corresponding to a higher image contrast. We calculate the local image contrast [4] for regions A and B, and the local image contrasts for our method are 20.7% and 20.8%, which are greater than those of 6.3% and 5.2% for Schechner's method. It also means that "Mueller Step-2" has a higher contrast than that of "Schechner Step-2" in terms of objective quantified metrics.

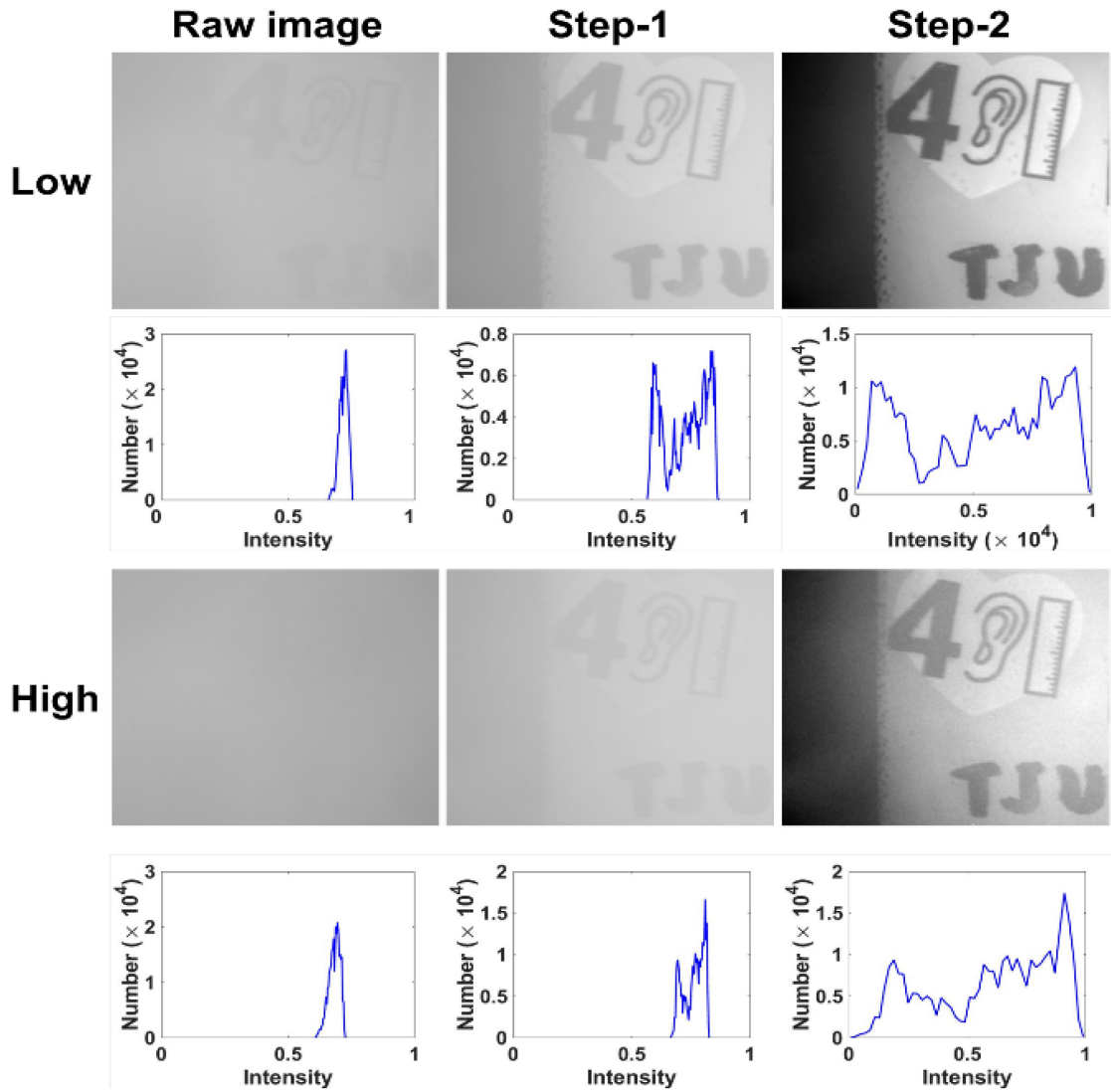


Fig. 5. Underwater image restoration results and the histograms in different turbidities of water.

TABLE I
COMPARATIVE ANALYSIS OF DIFFERENT METHODS

	EME	STD	Enhancement ratio
Raw image	0.294	0.019	\
Mueller Step-1	0.632	0.059	163%
Schechner Step-1	0.452	0.031	58%
Mueller Step-2	4.630	0.282	1430%
Schechner Step-2	3.719	0.183	1014%

In order to further evaluate the image quality and compare it with the traditional method in terms of other typical objective quantified metrics, we also calculate the values of measure of enhancement (EME) [2], [4] and the standard deviation (STD) [4], [26]. The corresponding values are shown in Table I. Then the average values of the enhancement ratios for EME and STD

compared with the raw image are also listed in the last column of Table I for the purpose of comparison.

In order to further verify the effectiveness of our method, we also perform experiments in different turbidities of water by blending the clear water with different volumes of milk, and the results are shown in Fig. 5. The concentrations of milk in water are 0.52 g/L and 0.69 g/L, and the maximum DoPs of them are 0.7969 and 0.7985 respectively. It can be seen that our method can effectively suppress the backscattered light and significantly enhance the image contrast with lower image distortion in different turbidities of water. In particular, even when the water is dense turbid with a high concentration of milk, the polarization filtering can also significantly suppress the backscattered light. Moreover, with post-processing, for example, histogram stretching, the image can eventually be clear enough to reveal the details of scenes. In addition, we also plot in Fig. 5 the histograms of corresponding images, which provide another perspective to analyze the image enhancement. It can be seen in the histograms that the raw images in turbid water

have a narrow distribution of gray levels. While by the proposed Mueller imager, the range of gray levels can be considerably extended. This is because the backscattered light is suppressed, and the details of the scene become visible. Furthermore, with the post-processing of histogram stretching, the gray level covers the whole range from 0 to 1, and the image becomes even clearer.

IV. CONCLUSION

In conclusion, we propose an image recovery method based on the Mueller polarimetric imager for underwater imaging. It enhances the image quality by optically filtering out the backscattered light. In particular, we synergistically modulate the states of PSG and PSA to remove the backscattered light in an optimal way, and consequently, the backscattered light in the images can be significantly suppressed. The foremost advantage of our method is that it is pure optical without digital processing, and thus there is less image distortion, which is beneficial for further image processing to finally achieve superior image quality. Besides, another attractive advantage of the proposed Mueller imager is the ability to realize the real-time clear vision if the underwater environment is stable without significant variation of the Mueller matrix of the turbid water. In practice, this assumption is valid if we capture the images in the shallow sea, or the water condition is relatively stable during a certain period of time. Of course, since the polarization property depends on various properties of the turbid media (such as particle sizes, shapes, and concentrations, etc.) [27], [28], investigating the corresponding effects on image quality enhancement is indeed an interesting perspective. Moreover, the method proposed in this paper can be generalized to color images by employing it for RGB channels, and finally, the RGB three-channel images can be combined into one color image. Of course, color distortion could be considered for the color images. The method we proposed has the effect of suppressing scattering in real-time for the underwater environment where the background scattering condition is stable.

REFERENCES

- [1] G. N. Bailey and N. C. Flemming, "Archaeology of the continental shelf: Marine resources, submerged landscapes and underwater archaeology," *Quaternary Sci. Rev.*, vol. 27, pp. 2153–2165, 2008.
- [2] F. Snik *et al.*, "An overview of polarimetric sensing techniques and technology with applications to different research fields," in *Proc. Polarization: Meas., Anal., Remote Sens. XI. Int. Soc. for Opt. Photon.*, 2014.
- [3] Y. Y. Schechner and N. Karpel, "Recovery of underwater visibility and structure by polarization analysis," *IEEE J. Ocean. Eng.*, vol. 30, no. 3, pp. 580–587, Jul. 2006.
- [4] X. Li *et al.*, "Polarimetric image recovery method combining histogram stretching for underwater imaging," *Sci. Rep.*, vol. 8, 2018, Art. no. 12430.
- [5] J. Guan and J. Zhu, "Target detection in turbid medium using polarization-based range-gated technology," *Opt. Exp.*, vol. 21, 2013, Art. no. 14152.
- [6] T. Treibitz and Y. Y. Schechner, "Active polarization descattering," *IEEE Trans. Pattern Anal. Mach. Intell.*, vol. 31, pp. 385–399, 2009.
- [7] M. R. Elsayed, Y. Zhao, and J. C. W. Chan, "Polarization guided autoregressive model for depth recovery," *IEEE Photon. J.*, vol. 9, no. 3, Jun. 2017, Art. no. 6803016.
- [8] J. Liang, L. Ren, E. Qu, B. Hu, and Y. Wang, "Method for enhancing visibility of hazy images based on polarimetric imaging," *Photon. Res.*, vol. 2, pp. 38–44, 2014.
- [9] F. Liu *et al.*, "Deeply seeing through highly turbid water by active polarization imaging," *Opt. Lett.*, vol. 43, pp. 4903–4906, 2018.
- [10] H. Hu, L. Zhao, X. Li, H. Wang, and T. Liu, "Underwater image recovery under the nonuniform optical field based on polarimetric imaging," *IEEE Photon. J.*, vol. 10, no. 1, Feb. 2018, Art. no. 6900309.
- [11] J. Guan, J. Zhu, H. Tian, and X. Hou, "Real-time polarization difference underwater imaging based on stokes vector," *Acta Physica Sinica*, vol. 64, 2015, Art. no. 224203.
- [12] H. Hu *et al.*, "Polarimetric image recovery in turbid media employing circularly polarized light," *Opt. Exp.*, vol. 26, pp. 25047–25059, 2018.
- [13] G. Lewis, D. Jordan, and P. Roberts, "Backscattering target detection in a turbid medium by polarization discrimination," *Appl. Opt.*, vol. 38, pp. 3937–3944, 1999.
- [14] J. Aval, A. Alfalou, and C. Brosseau, "Polarization signals in the marine environment," in *Proc. SPIE Int. Soc. for Opt. Eng.*, vol. 5158, 2003, pp. 85–92.
- [15] F. Liu, Y. Wei, P. Han, K. Yang, L. Bai, and X. Shao, "Polarization-based exploration for clear underwater vision in natural illumination," *Opt. Exp.*, vol. 27, pp. 3629–3641, 2019.
- [16] H. Tian, J. Zhu, S. Tan, Y. Zhang, Y. Li, and X. Hou, "Rapid underwater target enhancement method based on polarimetric imaging," *Opt. Laser Technol.*, vol. 108, pp. 515–520, 2018.
- [17] J. Aval, A. Alfalou, and C. Brosseau, "Polarization and hyperspectral imaging matter for newly emerging perspectives in optical image processing: Guest editorial," *Adv. Opt. Photon.*, vol. 11, pp. ED10–ED14, 2019.
- [18] P. Wang, Q. Chen, G. Gu, W. Qian, and K. Ren, "Polarimetric image discrimination with depolarization Mueller matrix," *IEEE Photon. J.*, vol. 8, no. 6, Dec. 2016, Art. no. 6901413.
- [19] M. Richert, X. Orlik, and A. Martino, "Adapted polarization state contrast image," *Opt. Exp.*, vol. 17, pp. 14199–14210, 2009.
- [20] X. Li, T. Liu, B. Huang, Z. Song, and H. Hu, "Optimal distribution of integration time for intensity measurements in stokes polarimetry," *Opt. Exp.*, vol. 23, pp. 27690–27699, 2015.
- [21] K. O. Amer, M. Elbouz, A. Alfalou, C. Brosseau, and J. Hajjami, "Enhancing underwater optical imaging by using a low-pass polarization filter," *Opt. Exp.*, vol. 27, pp. 621–643, 2019.
- [22] X. Li, B. L. Teurnier, M. Boffety, T. Liu, H. Hu, and F. Goudail, "Theory of autocalibration feasibility and precision in full stokes polarization imagers," *Opt. Exp.*, vol. 28, pp. 15268–15283, 2020.
- [23] M. Dubreuil, P. Delrot, I. Leonard, A. Alfalou, C. Brosseau, and A. Dogariu, "Exploring underwater target detection by imaging polarimetry and correlation techniques," *Appl. Opt.*, vol. 52, pp. 997–1005, 2013.
- [24] K. He, J. Sun, and X. T. "Single image haze removal using dark channel prior," *IEEE Trans. Pattern Anal. Mach. Intell.*, vol. 33, no. 12, pp. 2341–2353, Dec. 2011.
- [25] A. M. Reza, "Realization of the contrast limited adaptive histogram equalization (CLAHE) for real-time image enhancement," *J. VLSI Signal Process. Syst. Signal, Image Video Technol.*, vol. 38, pp. 35–44, 2004.
- [26] H. Z. Nafchi, S. Atena, R. Hedjam, and C. Mohamed, "Mean deviation similarity index: Efficient and reliable full-reference image quality evaluator," *IEEE Access*, vol. 4, pp. 5579–5590, 2016.
- [27] F. Shen, B. Zhang, K. Guo, Z. Yin, and Z. Guo, "The depolarization performances of the polarized light in different scattering media systems," *IEEE Photon. J.*, vol. 10, no. 2, Apr. 2018, Art. no. 3900212.
- [28] Q. Xu *et al.*, "Transmitting characteristics of polarization information under seawater," *Appl. Opt.*, vol. 54, pp. 6584–6588, 2015.
- [29] C. Brosseau, *Fundamentals of Polarized Light*. Wiley-Interscience, 2015.
- [30] D. Bicout, C. Brosseau, A. S. Martinez, and J. M. Schmitt, "Depolarization of multiply scattered waves by spherical diffusers: Influence of the size parameter," *Phys. Rev. E.*, vol. 49, no. 2, pp. 1767–1770, 1994.